GNC 2011
8th International ESA Conference on Guidance, Navigation & Control Systems
Karlovy Vary, Czech Republic 5 - 10 June 2011
European Space Agency

HARDWARE-IN-THE-LOOP RENDEZVOUS SIMULATION USING A VISION BASED SENSOR

T. Boge[1], H. Benninghoff[1], T. Tzschichholz[1,2]
[1]German Aerospace Center (DLR), Germany
[2]University of Wuerzburg, Germany.

ABSTRACT

One of the critical issues of a satellite On-Orbit Servicing (OOS) mission is to ensure a safe and reliable Rendezvous and Docking (RvD) process. This most risky part of the mission must be carefully analyzed, simulated and verified before the mission can be launched.

This paper focuses on the utilization of the new RvD simulation facility called EPOS 2.0 (European Proximity Operations Simulator) to establish a hardware-in-the-loop (HIL) simulation of a close-range rendezvous process. As navigation sensor a monocular camera is used to measure the relative position and orientation of a mock-up of a Geo-stationary target satellite. A new developed image processing algorithm tracks the outer edges of the satellite body under different illumination conditions. The complex software functionality for relative guidance, navigation and control (GNC) and for the satellite dynamics is developed under Matlab/Simulink environment and auto-coded with Real Time Workshop.

1. INTRODUCTION

A. ON-ORBIT SERVICING

Meanwhile, On-Orbit Servicing (OOS) has become part of the space programs of the US, Japan, Canada and Germany. A milestone was set with the successful completion of DARPA's Orbital Express [1] (OE) mission in 2007. The goal of OE was to demonstrate the ability to autonomously perform Rendezvous & Docking (RvD) operations including maintenance activities like refueling. In contrast to the goals of OE, the focus of DLR is to capture non-cooperative and/or not specially prepared client spacecraft. "Non-cooperative" is understood as there is no cooperation with respect to attitude and orbit control of the client, e.g. when the client is out of operation. "Not specially prepared" means that the client satellite does not have a special docking port or retro reflectors used for vision based navigation.

The paper is based on the following two reference mission scenarios where DLR is involved.

The OLEV mission is a purely commercial project managed by a European consortium including a strong DLR participation. The business case of OLEV is to build an orbital servicer which is able to dock on high value, geostationary communication satellites and to take over attitude and orbit control in order to extend the clients lifetime after its fuel has been depleted (see fig. 1) Beside life extension OLEV can be used for fleet management purposes like relocation to other GEO positions or disposal to graveyard orbit.

The navigation concept of OLEV is to use ranging for absolute navigation and to hand over to relative navigation at the distance of a two kilometer. For relative navigation a set of six rendezvous cameras (far, mid and close range, redundant) is used.

The OLEV project has finished a delta phase B study; the present focus lies on financial engineering.

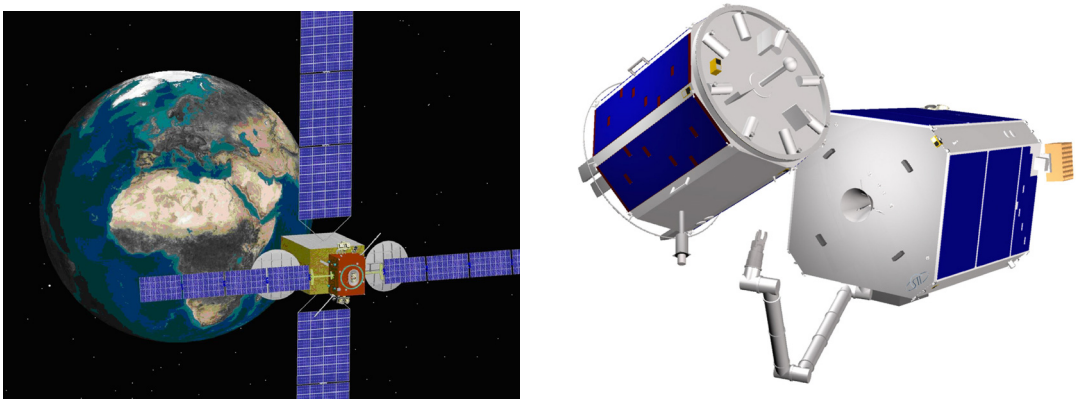

Fig. 1: *SMART-OLEV docked at (left) and Servicer and client satellite of DEOS Mission (right) [13]*

In opposite to OLEV the DEOS mission is a technology demonstration of German On-orbit servicing capabilities. The primary goals of the DEOS are:
(1) to capture a tumbling non-cooperative client satellite with a servicer spacecraft and
(2) to de-orbit the coupled configuration within a pre-defined orbit corridor at end of mission.
Secondary goals are to perform several rendezvous, capture and docking scenarios as well as orbit maneuvers with the mated configuration (see Figure 1).
For DEOS the expression "non-cooperative client" has to be understood in a sense that the client shall simulate a non-cooperative client. This means the client has no markers or retro reflectors for navigation purposes and the AOCS is switched off during the docking or grasping process. For the nominal rendezvous navigation a vision based sensor system is used (mono/stereo cameras / LIDAR).
The DEOS project started last year a phase B study financed by the German Space Agency.

B. NEW TECHNOLOGICAL CHALLENGES

For the new OOS missions the following new technological requirements can be found:
(A) the rendezvous phase
Typically the target satellites have not been built for rendezvous and docking tasks. Therefore the rendezvous sensors and systems have to cope with completely uncooperative targets.
(B) the docking phase
The robotic based mechanisms have to ensure a safe and reliable gripping or docking at a target without any foreseen docking mechanisms.
(C) the degree of autonomy
For missions without continuous contact to ground (typically LEO missions), the on-board autonomy plays an important role.
(D) Simulation on ground
One of the challenges of such OOS missions is to ensure a safe and reliable rendezvous and docking (RvD) process. Especially this phase has to be analyzed, simulated and verified in detail. Classical approaches e.g. numerical simulations deliver only limited results. Therefore simulation procedures, tests and the appropriate testing facilities have to be defined allowing simulation of the entire RvD process.
This paper focuses only on point (A) and (D). Chapter 2 delivers a short introduction into the new rendezvous and docking simulator EPOS 2.0. Afterwards the DLR developments of a rendezvous GNC-system are described which is using a vision based sensor. Finally these new GNC-system is tested performing HIL-simulations on the new facility, EPOS 2.0.

C. RELATED WORK

There have been several examples of simulators for simulating rendezvous and docking operations of space systems. German Aerospace Center (DLR) and ESA developed a simulation facility called European Proximity Operations Simulator (EPOS), a former version of the new EPOS 2.0 facility introduced in this paper, two decades ago for simulating satellite rendezvous operations [2]. The facility was used to support the testing of ATV and HTV rendezvous sensors. NASA/MSF developed an HIL simulator using a 6-DOF Stewart platform for simulating the Space Shuttle being berthed to the International Space Station (ISS) [3,4]. The Canadian Space Agency (CSA) developed an SPDM Task Verification Facility (STVF) using a giant 6-DOF, customer-built, hydraulic robot to simulate SPDM performing contact tasks on ISS [5,6]. US Naval Research Lab used two 6-DOF robotic arms to simulate satellite rendezvous for HIL testing rendezvous sensors [7]. China is also developing a dual-robot based facility to simulate satellite on orbit servicing operations [8]. The unique features of the new EPOS facility, in comparison with those existing systems, are that it uses two heavy-payload industrial robots which can handle a payload up to 200 kg and it allows one robot to approach the other from 25-meter distance away until zero distance.
In addition to the work for RvD simulation there have been published a lot of papers concerning vision based GNC developments. For instance, [11] suggests an image processing algorithm which detects a no cooperative target object in an image. A complete GNC system based on a stereo camera system is proposed in [9]. An approach similar to ours was made in [10] using a monocular camera to detect and control a target satellite.

2. EPOS 2.0 – A NEW SIMULATOR FOR RENDEZVOUS AND DOCKING

A. OVERVIEW

Future applications for satellite on-orbit servicing missions require the EPOS facility to be able to provide the following test and simulation capabilities:

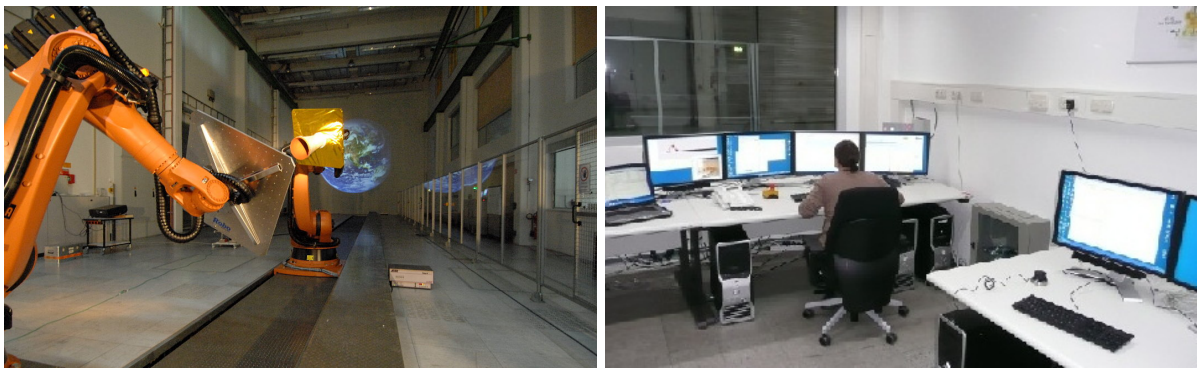

Fig. 2: *The new EPOS facility: robotics-based testbed (left) and operation station (right)*

(A) the 6-DOF relative dynamic motion of two satellites in the final approaching phase from 25 meters to 0 meters.
(B) the 6-DOF contact dynamic behavior during the entire docking process including the initial impact, soft docking, and hard docking (final rigidization).
(C) the space-representative lighting and background conditions

The new EPOS facility is aimed at providing test and verification capabilities for complete RvD processes of on-orbit servicing missions. The facility comprises a hardware-in-the-loop simulator based on two industrial robots (of which one is mounted on a 25m rail system) for physical real-time simulations of rendezvous and docking maneuvers. This test bed will allow simulation of the last critical phase (separation ranging from 25m to 0m) of the approach process including the contact dynamics simulation of the docking process.
Moreover, its main advances are:

- It is a highly accurate test bed. The measurement and positioning performance will be increased by factor 10 compared to the former EPOS facility.
- Dynamical capabilities will allow for high commanding rates and the capability of force and torque measurements.
- The simulations of sunlight illumination conditions as well as the compensation of Earth-gravity force are both part of the assembly to generate an utmost realistic simulation of the real rendezvous and docking process.
- The utilization of standard industrial robotics H/W allows a very high flexibility related to different application scenarios.

The new facility consists of the following components [12]:

- A rail system mounted on the floor to move an industrial robot up to a distance of 25m,
- A KUKA KR240 robot (robot 1) mounted at the end of the rail system for simulating the 6 degree of freedom of the second spacecraft.
- A KUKA KR100HA robot (robot 2) mounted on the rail system for simulating the 6 degree of freedom of one spacecraft.
- A PC-based monitoring and control system to monitor and control the RvD simulation on the facility.

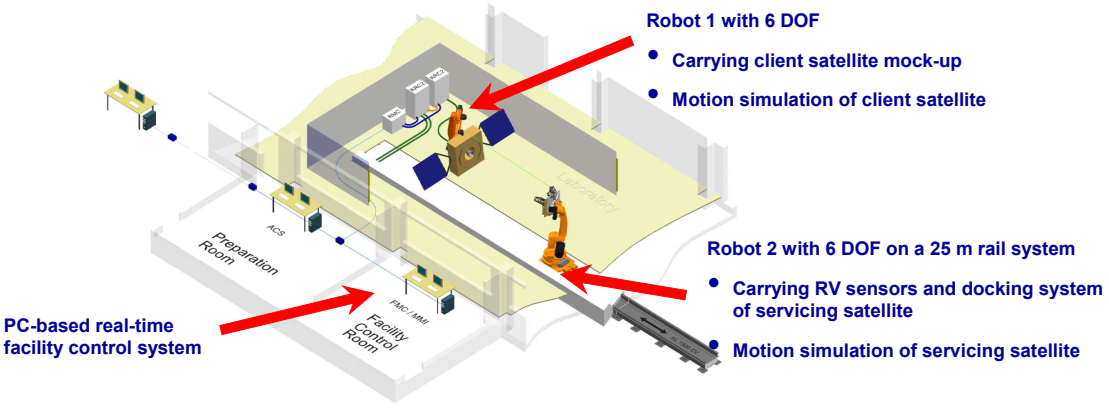

Fig. 3: *Components of the new testbed – EPOS 2.0*

Table 1: *EPOS motion capabilities [12]*

Parameter	Robot 1	Robot 2
Position:		
X [m]	-2,5 - +2,5	-2,5 - +24,5
Y [m]	-1,0 - +4,0	-2,5 - +2,5
Z [m]	-0,5 - +1,5	-0,5 - +1,2
Attitude:		
Roll [deg]	-300 - +300	-300 - +300
Pitch [deg]	-90 - +90	-90 - +90
Yaw [deg]	-90 - +90	-90 - +90
Max. tip velocity:		
Translational [m/s]	2	2
Rotational [deg/s]	180	180
Command IF		
Command rate [Hz]	250	250
First natural frequency [Hz]	8-10	8-10

B. CAPABILITIES AND PERFORMANCES

Table 1 summarizes the EPOS motion simulation capabilities and performances.
Because EPOS will be used for RvD sensor verification purposes, the facility was extensively calibrated after its installation. With a laser tracker device an overall positioning accuracy of the facility of better than 2 mm (3D, 3σ) and an orientation accuracy of 0.2 deg (3D, 3σ) have been verified.
In addition, it is planned to develop an online measurement system that measures the relative position between both robots and commands corrections to the robots. So the achieved position accuracy is expected in the submillimeter range. Furthermore, a lot of effort was made to increase the command frequency to 250 Hz, which is an important precondition to simulate real-time contact dynamics.

3. HARDWARE-IN-THE-LOOP SIMULATION FOR RENDEZVOUS PROCESSES

A. SIMULATION CONCEPT

Hardware-in-the-loop simulation is a very effective way to perform verification and testing of complex real-time embedded systems like rendezvous sensors. Inputs and outputs of an embedded system (here: a mono, CCD camera) are connected to a correspondent counterpart - the so-called HIL-simulator - that simulates the real environment of the system.

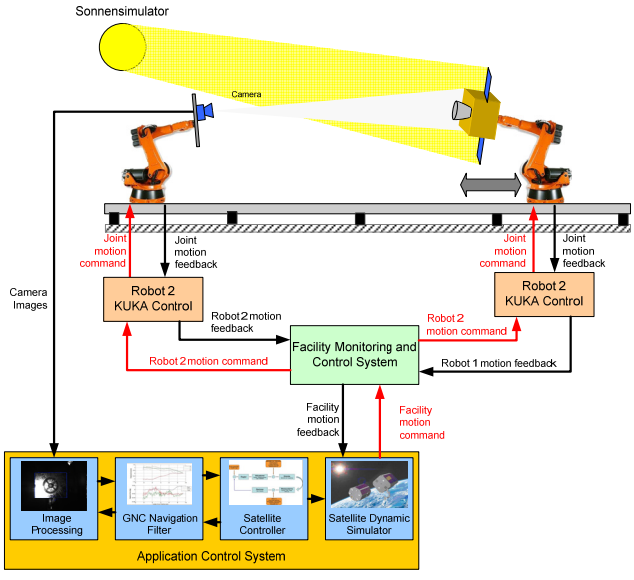

Fig. 4: *Control loop for rendezvous*

Table 2: *Clohessy Wiltshire coordinate framework*

x	V-Bar	Tangential direction, i.e. the direction of the orbital velocity vector
y	H-Bar	Opposite direction of the angular momentum vector of the orbit, i.e. parallel to the normal vector of the orbit plane
z	R-Bar	Direction to earth, i.e. radial from the spacecraft's center of mass to the centre of the Earth

A typical HIL setting for rendezvous simulation is as follows: A rendezvous sensor for relative navigation measures relative position and attitude of the servicing satellite with respect to the target satellite. Based on this measurement thruster commands are computed by comparison of the actual position and attitude with the reference guidance values. Control commands for actuators like thrusters or reaction wheels cannot be simulated with real hardware. However the computation of forces and torques can be used to determine the position and attitude numerically based on equations of motion for the satellites' orbit and attitude. In the next sample, the computed positions and attitudes are commanded to the facility.
The main task in rendezvous simulation is to develop a stable control loop for orbit and attitude control. Fig. 4 shows a typical control loop for a rendezvous scenario including sensor system, guidance, navigation and control functionality, actuators and the satellites' dynamics, kinematics and their environment.
The state, i.e. relative position and attitude, is simulated by the manipulators of the EPOS facility. The manipulator can be regarded as the connection of the numerical HIL-simulator with the embedded system, i.e. with the rendezvous sensor.
In the following section the dynamical models, the navigation sensor and the GNC system are described in detail. Finally, an overview on technical aspects concerning development of real-time rendezvous simulation software is given.

B. DYNAMICAL AND KINEMATICAL SPACECRAFT MODELS

The objective is to develop a realistic simulation of the rendezvous process including the real orbit mechanics. A numerical model is implemented to emulate the realistic motion of the satellites in orbit. For orbit control position and velocity are calculated in the Clohessy Wiltshire (CLW) coordinate framework. Table 2 shows the used conventions [14]:
The origin of the CLW coordinate framework is aligned with the center of mass of the target spacecraft. So the chaser's position is seen in the local orbital frame of the target.
The Hill equations [14] are used to describe the chaser's relative translational motion in the local reference system of the target. The equations of motion are a system of linear ordinary differential equations:

$$\begin{aligned} \ddot{x} &= 2\omega_0 \dot{z} + \frac{1}{m} f_x \\ \ddot{y} &= -\omega_0{}^2 y + \frac{1}{m} f_y \\ \ddot{z} &= -2\omega_0 \dot{x} + 3\omega_0{}^2 z + \frac{1}{m} f_z \end{aligned} \tag{1}$$

f is the sum of control and disturbance forces acting on the chaser satellite. The activation of thrusters and the simulation of the real orbit mechanics are done numerically by solving the equations of motions. The computed position and attitude is then commanded to the facility.
The spacecraft attitude is described by Euler angles and quaternions. Here the Euler angles (φ, θ, ψ) convention '123' is used, i.e. an orientation described by the angles consists of three consecutive rotations: First a rotation around the x-axis with angle φ, then a rotation around the resulting y-axis with angle θ and finally a rotation around the resulting z-axis with angle ψ.
The attitude kinematics of chaser and target are each given by the quaternion differential equation [15]:

$$\dot{q} = \frac{1}{2} \Omega q \tag{2}$$

whereas

$$\Omega = \begin{pmatrix} 0 & \omega_z & -\omega_y & \omega_x \\ -\omega_z & 0 & \omega_x & \omega_y \\ \omega_y & -\omega_x & 0 & \omega_z \\ -\omega_x & -\omega_y & -\omega_z & 0 \end{pmatrix} \tag{3}$$

Fig. 5: *Prosilica Gigabit Ethernet vision camera (GC-655)*

The attitude dynamics can be expressed by Euler equation [15]:

$$I\dot{\omega} = t - \omega \times I\omega \tag{4}$$

Here, t denotes the sum of control and disturbance torques. Both, quaternion and Euler equation are a system of non-linear differential equations.
For solution of the orbit and attitude dynamic models Euler method with a time step of 0.004s is used. This is the sample time the facility requires. The current configuration on EPOS restricts every Simulink application to use Euler method as solver for ordinary differential equations.

C. VISION-BASED NAVIGATION SENSOR

As vision sensor a Prosilica Gigabit Ethernet vision camera (GC-655) has been used to measure the relative position and attitude (pose), see Fig. 5. In detail, it is a monochromatic, VGA-resolution (640x480) charge coupled device (CCD) sensor with large pixels on the chip, to increase sensitivity [13]. The sensor chip has a very high dynamic range to cover various lighting situations.
Image processing algorithms then determine the pose of the target object in real-time. Since only a single camera is used, additional information about the target is necessary to obtain full 6-DOF pose estimation. I.e. it is an algorithm to track a previously identified object. In the rendezvous simulations presented in this paper a rectangular target with known edge lengths is assumed.
Due to the real-time constraint, an edge tracking approach has been chosen that relies on contrast and texture. Depending on the local surface properties, the appropriate method is selected autonomously. Usually the fast Sobel filter [16] which uses changes in the brightness is applied. However, if the image is noisy or the local contrast is weak, the texture segmentation [17] is preferable which evaluates changes in the surface texture to detect edges.
The image processing algorithm (see Fig. 6 for an illustration) consists of the following steps:

(1) Initialization: Calculation of initial corner positions: the pose estimation of the last time step is used to get an initial guess of the corner points assuming that there are only small changes in the pose between two corresponding time steps. The old pose is projected to the 2D image frame using a pinhole camera model. Virtual edge lines are constructed by connecting the 2D corner points.
(2) Constructing scanlines and scanning for edges along the scanlines: The update of the edge lines relies on so-called scanlines. These are strips of pixels which are perpendicular with respect to an anticipated edge. The Sobel filter or the texture segmentation method is then applied to retrieve the intersection point of the scanline and the real edge. This is the point along the scanline where a change in the brightness or a change in the surface texture appears. For each edge, several scanlines are evaluated.

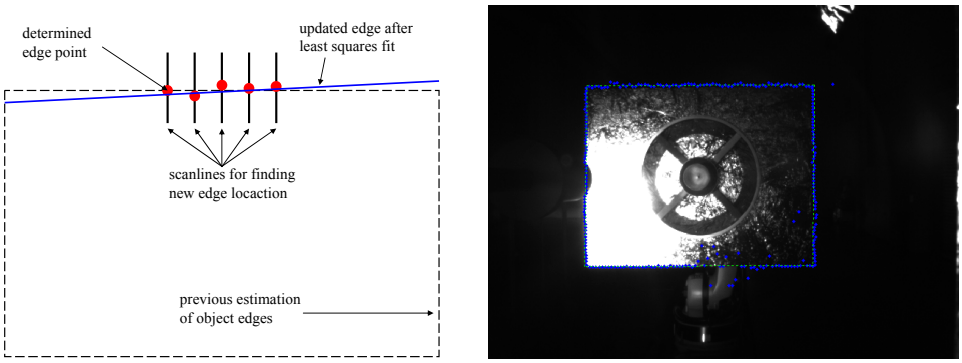

Fig. 6: *Illustration of the edge tracking algorithm (left) and tracking edges of client mock-up (right) [13]*

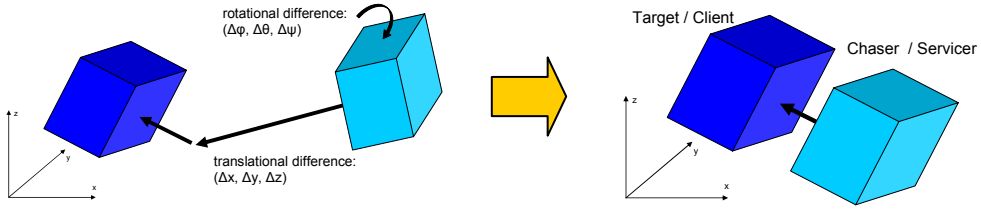

Fig. 7: *Chaser guidance with respect to client*

(3) Performing line fits: A stable point set is retrieved from the set of intersection points by removing outliers. Therefore the RANSAC [18] algorithm is applied. Using the set of stable points a line fit is performed to get an estimation of the new edges and finally an estimation of the new corner points in the 2D image coordinate frame.

(4) Update of the pose vector: The Levenberg-Marquardt [19] optimization method is applied to get 6-DOF pose estimation by minimizing the projection residual. I.e. the least squares fit searches for the pose that minimizes the sum of squares of the difference between the model corner points (depending on the pose) and the detected, measured corner points.

In addition Fig. 6 shows a picture of the client mock-up and the detected edges (green, dotted line) as well as the set of detected intersection points (blue). One can observe some outliers. However, they are removed by the RANSAC algorithm [18].

D. GUIDANCE, NAVIGATION AND CONTROL FUNCTIONALITY

The GNC functions are implemented as software in the automated onboard computer of the chaser satellite. They use the measurements delivered by the vision-based rendezvous sensor to calculate commands for the actuators (e.g. thrusters). A rendezvous approach requires a continuously control of trajectory and attitude [15].

GUIDANCE

The developed rendezvous simulation contains a guidance subsystem which provides reference values for the state at each sample time to generate a position and attitude profile [15]. The objective of guidance is to define and force a state that the spacecraft should finally reach.

Currently, several guidance modes are implemented. For an approach e.g. from 20m to 3m the guidance trajectory consists of three phases: An acceleration phase to reach a desired velocity, a phase of constant velocity and finally a deceleration phase.

For tests of the first prototype of the rendezvous software a guidance mode is used which delivers constant reference values. This mode can also be applied to simulate the behavior at hold points.

The chaser guidance function additionally concerns the client's rotational movement. The chaser has to react to changes in the client's attitude to keep the desired relative orientation and position with respect to the tumbling target spacecraft. Fig. 7 shows an example: The servicer should take a defined position and orientation with respect to the target surface, i.e. it should reach a pre-defined distance (e.g. 1m) to the target and the body axes of the chaser should be aligned with those of the target.

NAVIGATION

The image processing delivers a measurement of the client's position and attitude with respect to the camera. This pose estimation can be used for relative navigation concerning the servicing satellite.

A navigation filter for orbit estimation is implemented and integrated in the orbit control loop as shown in Fig. 4. The filter provides an estimate for the relative position of the servicer.

The servicer's absolute position and attitude is assumed to be known, i.e. provided by some other accurate attitude sensor like star sensors, gyroscope, etc. The measured client position and attitude with respect to the chaser is smoothed by a filter.

The task of a navigation filter is to provide the controller with the necessary information about the current position and attitude of the target spacecraft. The objective of all filters is to calculate an estimation of the state vector which is an optimum based on measurements and additional information e.g. the dynamic behavior of the physical process. For rendezvous simulation described in this paper a Kalman filter is implemented which tries to minimize the variance of the estimation error [14, 15, 20].

The Kalman filter assumes the system dynamics and the measurement equations to be linear [15]. Expressed in state-space [20] form the linear equations of motions can be written as

$$\dot{x} = Fx + Gu + N\nu \tag{5}$$

x is the state vector which has to be estimated. The control vector u could be delivered by the controller. The system dynamics matrix F, the control matrix G and the matrix N are known. ν is an additive, zero mean, white Gaussian noise which describes the uncertainty of the process model. To simplify the notation the time dependency of the quantities has been neglected in (5).
The Hill equations (1) can be rewritten in that form. We set the state vector to $x = (p, \dot{p}) \in IR^6$, where p is the relative position vector and $\dot{p}$ is the velocity vector and $u = (f) \in IR^3$ where f is sum of control and disturbance forces acting on the chaser satellite. These results in the following matrix definition:

$$F = \begin{pmatrix} 0 & 0 & 0 & 1 & 0 & 0 \\ 0 & 0 & 0 & 0 & 1 & 0 \\ 0 & 0 & 0 & 0 & 0 & 1 \\ 0 & 0 & 0 & 0 & 0 & 2\omega_0 \\ 0 & -\omega_0^2 & 0 & 0 & 0 & 0 \\ 0 & 0 & 3\omega_0^2 & -2\omega_0 & 0 & 0 \end{pmatrix} \tag{6}$$

$$G = \frac{1}{m}\begin{pmatrix} 0 & 0 & 0 \\ 0 & 0 & 0 \\ 0 & 0 & 0 \\ 1 & 0 & 0 \\ 0 & 1 & 0 \\ 0 & 0 & 1 \end{pmatrix} \tag{7}$$

Where ω_0 is the orbit rate and m is the satellite mass.
The Extended Kalman filter (EKF) generalizes the concept of Kalman filtering to nonlinear system dynamics. It can be applied for systems of nonlinear differential equations:

$$\dot{x} = f(x, u, t) + N\nu \tag{8}$$

where f is a nonlinear function [20]. A first-order approximation of (8) is used. The system dynamics matrix at time t is set to

$$F(t) = \left.\frac{\partial f}{\partial x}\right|_{x = x(t - \Delta t)} \tag{9}$$

The equations of motion which model the attitude kinematics and dynamics are non-linear. The EKF is applied setting the state vector to $x = (\alpha, \omega) \in IR^6$ where $\alpha = [\varphi, \theta, \psi]^T$ is a vector of Euler angles which describing the client attitude and ω is the client satellite body rate vector and $u = (t) \in IR^3$ where t is sum of control and disturbance torques. While F has to be calculated according (9), the matrix G can be computed as following:

$$G = I^{-1} \cdot \begin{pmatrix} 0 & 0 & 0 \\ 0 & 0 & 0 \\ 0 & 0 & 0 \\ 1 & 0 & 0 \\ 0 & 1 & 0 \\ 0 & 0 & 1 \end{pmatrix} \tag{10}$$

Both filters, the orbit and the attitude filter, use the following linear, discrete measurement model:

$$z = Hx + w \tag{11}$$

w is the measurement noise, assumed to be an additive, zero mean, white Gaussian noise. The measurement matrix for the both filter results in:

$$H = \begin{pmatrix} 1 & 0 & 0 & 0 & 0 & 0 \\ 0 & 1 & 0 & 0 & 0 & 0 \\ 0 & 0 & 1 & 0 & 0 & 0 \end{pmatrix} \tag{12}$$

State estimation with Kalman filtering consists of consecutive cycles with predictor and corrector steps. During the prediction step the state is propagated whereas in the correction step the predicted values are updated using measurement of the state delivered by the rendezvous sensor. Propagation is based on numerical determination of the present state using dynamic satellite models. If no measurements are available - for example during intermediate steps if filter and sensor run with different sample times - one can use pure propagation for state estimation.
A major challenge is the filter tuning, i.e. appropriate assumptions of the covariance's of the noise vectors v and w. By setting these covariance's one can influence the weighting of the measurement update.

CONTROL

The development of all the components of the control loop is ongoing. At present time there does not exist any detailed performance evaluation of all these components. Especially the nonlinear errors or influences and the occurring time delays inside the loop are difficult to handle by any type of controller. Therefore the first main objective is to get a stable system.
Based on the model of the dynamic motion of the two spacecrafts (see chapter 3.B.) the plants for the orbit and attitude controller are approximated by an integral element of second order (I2 element). The cross correlations will be disregarded for this assumption. Such an unstable plant can be stabilized by a conventional PD controller [15]. The resulting control loop structure is shown in Fig. 8.
The corresponding controller gains k_P and k_D were calculated based on the desired steady state performance requirements and the desired damping of the entire system [15].
After evaluation of all loop components a more advanced controller will be designed to achieve the best system performance.

E. DEVELOPMENT OF REAL-TIME SIMULATION SOFTWARE

MATLAB and the MATLAB related tool Simulink are used as development environment for rendezvous software. Simulink is a model-based simulation tool which is integrated in the MATLAB environment and it is a widely used tool in control theory domain.
Interfaces to additional hardware components (e.g. the camera as rendezvous sensor) have been established. Image processing, navigation filter, control algorithms and the dynamic satellite simulator are integrated in the Simulink model.
Additionally, multi-tasking execution of the model is supported (table 3). The satellites' dynamics run with a frequency of 250Hz which is the commanding frequency the facility requires. Therefore position and attitude commands are sent to the facility every 4ms. Other components with higher computational effort like the image processing are executed with a lower frequency. Tasks with lower frequency are assigned with a lower priority. They can be preempted by tasks with higher priority.

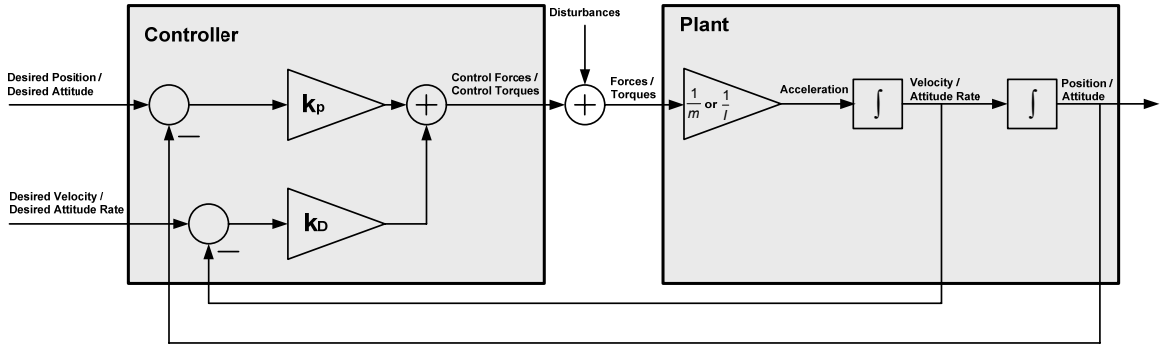

Fig. 8: *Chaser guidance with respect to client*

Table 3: *Frequencies of multi-tasking execution of the model*

Function	Frequency
Camera	5 Hz
Image Processing	5 Hz
Filter Corrector Step	5 Hz
Filter Propagation / Predictor Step	10 Hz
Controller	10 Hz
Satellite dynamics & kinematics	250 Hz

C source code for real-time execution of the model is generated by MATLAB Real-time workshop which is an additional tool for automatic code generation. The final executable runs on a real-time computer with the real-time operational system VxWorks. The MATLAB-Simulink interface allows to process simulation results offline using some of the MATLAB visualization or matrix/vector computing tools.

4. RESULTS

A. OVERVIEW

First tests of the rendezvous HIL-simulation have been performed on EPOS testing the behavior at discrete distances (hold points) and during an approach from 20m to 3m. Therefore, several guidance modes are used. Furthermore the rendezvous sensor and its performance are tested in a closed-loop application. In the past only offline tests were performed: Trajectories were generated on EPOS and sequences of images were captured and offline processed [13]. Presently, the sensor is integrated in a dynamic simulation with the real orbit mechanics and an implemented GNC system. The entire rendezvous control system has proved to be stable.
Table 4 presents the main parameters of the simulation: the sensor parameters, the satellite data, the covariance assumptions used in the navigation filter as well as the sample rates of the individual subsystems of the model.

B. NAVIGATION ANALYSIS

The following analysis has been done exclusively on geometrical projection of the target on the camera CCD sensor. These results can be used to calculate the order of magnitude of the expected error of the position and attitude determination algorithms based on a camera sensor. In addition it delivers a mathematical description about the influencing variables and their impact on the result, for instance the determination error evolution depending on the distance (range) to the target. This analysis can't replace the evaluation of the image processing software because it is a simplification of the complex measurement process, for instance the software uses in minimum the four corner points of the tracked satellite surface for position and attitude determination and can calculate average values.
The navigation performance of position estimation can be well analyzed using the geometric relations as shown in Fig. 9 (left side). This results in the following mathematical relation:

Table 4: *Simulation parameters*

Camera parameters:	
focal length in pixels	604
pixel grid size in [m]	$9.9 * 10^{-6}$
resolution in pixels	640 x 480
Satellite parameters:	
mass (servicer, client) in [kg]	1000
moment of inertia (servicer, client) in [kg m^2]	(100, 200, 80)
orbit rate (for LEO orbit) in [rad s^{-1}]	0.001
Dimensions of tracked satellite surface [m]	1.8 x 2.3
Filter parameters:	
Position:	
covariance of process noise v in [m]	$10^{-8} * I_{3x3}$
covariance of measurement noise w in [m]	$10^{-2} * I_{3x3}$
Attitude:	
covariance of process noise v in [rad]	$0.25*10^{-8} * I_{3x3}$
covariance of measurement noise w in [rad]	$(20* pi/180)^2 * I_{3x3}$

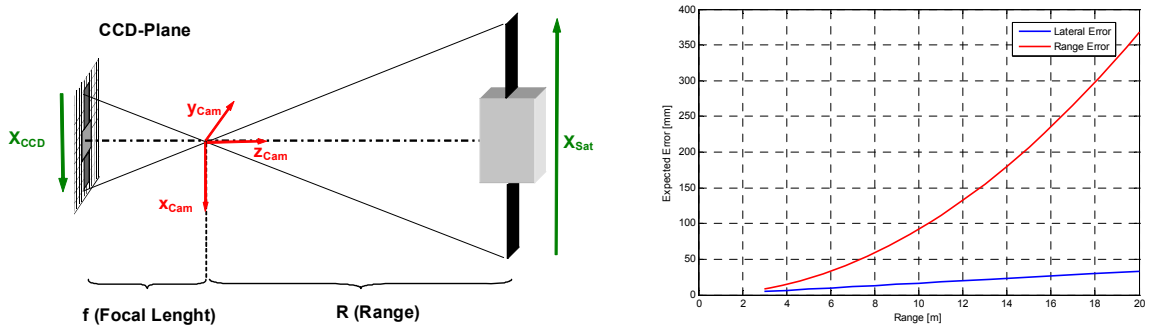

Fig. 9: *Navigation analysis for expected position error*

$$\frac{X_{CCD}}{f} = \frac{X_{Sat}}{R} \tag{13}$$

If we define X_{CCD} is the required measurement parameter in the image the partial derivations are:

$$\frac{\partial x_{CCD}}{\partial x_{Cam}} = \frac{f}{R}; \quad \frac{\partial x_{CCD}}{\partial z_{Cam}} = -\frac{fX_{Sat}}{R^2} \tag{14}$$

Based on (14) the order of magnitude of resulting lateral error (∂x_{Cam}) and range error (∂z_{Cam}) can be pre-estimated if we transform (14) to:

$$\left|\partial x_{Cam}\right| = \frac{R}{f}\partial x_{CCD}; \quad \left|\partial z_{Cam}\right| = \frac{R^2}{fX_{Sat}}\partial x_{CCD} \tag{15}$$

For a one pixel error (∂x_{CCD}) assumption the resulted position error is shown in Fig. 9 on the right side using the simulation parameter described in table 4.
The navigation performance of attitude estimation following in principle the same geometric relations as shown in Fig. 10 (left side). Here, α represents the roll attitude and β represents the pitch and yaw attitude of the target satellite. This results in the following mathematical relation:

$$\frac{X_{CCD}}{f} = \frac{X_{Sat}\sin(\alpha)}{R} \text{ and } \frac{X_{CCD}}{f} = \frac{X_{Sat}\cos(\beta)}{R} \tag{16}$$

The partial derivations are:

$$\frac{\partial x_{CCD}}{\partial \alpha} = \frac{fX_{Sat}}{R}\cos(\alpha) \text{ and } \frac{\partial x_{CCD}}{\partial \beta} = -\frac{fX_{Sat}}{R}\sin(\beta) \tag{17}$$

Based on (17) the order of magnitude of resulting attitude error can be pre-estimated if we transform (17) to:

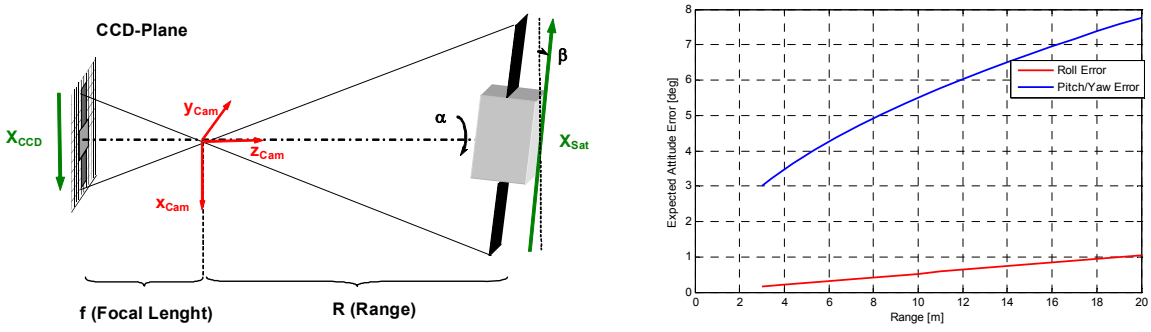

Fig. 10: *Navigation analysis for expected attitude error*

$$|\partial\alpha| = \frac{R}{fX_{Sat}\cos(\alpha)}\partial x_{CCD} \text{ and } |\partial\beta| = \frac{R}{fX_{Sat}\sin(\beta)}\partial x_{CCD} \tag{18}$$

For small angles (α, β <10deg) is $\cos(\alpha) \approx 1$ and $\partial\beta \approx \sin(\beta)$, (18) results in:

$$|\partial\alpha| = \frac{R}{fX_{Sat}}\partial x_{CCD} \text{ and } |\partial\beta| = \sqrt{\frac{R}{fX_{Sat}}\partial x_{CCD}} \tag{19}$$

For a one pixel error (∂x_{CCD}) assumption the resulted attitude error is shown in Fig. 10 on the right side using the simulation parameter described in table 4.

C. NAVIGATION SIMULATION RESULTS AT DIFFERENT HOLD POINTS

The navigation performance can be well investigated at discrete distances where one can analyze the errors of the single components. For this purpose a constant guidance mode is used.
In the following results of four demo tests are presented. The tests have been executed at an initial distance of 5m, 10m, 15m and 20m between chaser and target. Fig. 11 and Fig. 12 show the error of orbit and attitude estimation, i.e. the difference between real values and estimates. Errors in the measurement (red) as well as errors in Kalman Filter estimates (blue) are plotted.
Regarding the position the noise in the x -coordinate is bigger compared to the y - and z -component of the position vector as espected. The x -axis represents the approaching axis. Small changes in the distance are difficult to detect for the vision-based sensor because they could just cause sub-pixel changes in the image. However changes in the other translational coordinates are easier to recognize. For the same reason the error in the pitch and yaw component of the attitude are around one magnitude bigger than the error of the roll component.
Table 5 gives an overview of the root mean square error (RMSE) of the Kalman filter and the image processing measurement of position and attitude. It can be compared to the expected errors based on the geometrical analysis.
The root mean square error increases with the distance between chaser and target. However the order of magnitude is as expected if we assume a one pixel error of the image processing software. The range measurements and the attitude measurements are by factor 2-4 better then expected. This could be caused by using more than two points in the image for calculating the position and attitude.
From Fig. 11 and Table 5 we can observe the smoothing of the noise by the Kalman filter. Regarding the attitude the filter even reduces the measurement noise by factor 10.

Table 5: *Root Mean Square Navigation Errors and Expected Errors*

		5m	10m	15m	20m
Position:					
Filter:	X in [mm]	5.1	13.7	42.4	61.8
	Y in [mm]	2.7	9.7	16.9	22.0
	Z in [mm]	4.7	12.4	25.8	42.0
Measurement:	X in [mm]	6.4	27.2	71.1	123.6
	Y in [mm]	3.6	11.2	23.7	31.7
	Z in [mm]	10.5	13.4	31.5	48.3
Expected:	X in [mm]	22.9	91.9	206.9	367.9
	Y in [mm]	8.2	16.5	24.8	33.1
	Z in [mm]	8.2	16.5	24.8	33.1
Attitude:					
Filter:	Roll in [deg]	0.006	0.019	0.041	0.069
	Pitch in [deg]	0.107	0.321	0.254	0.455
	Yaw in [deg]	0.028	0.166	0.088	0.105
Measurement:	Roll in [deg]	0.084	0.154	0.225	0.371
	Pitch in [deg]	0.915	2.321	4.535	6.505
	Yaw in [deg]	0.412	1.676	3.123	4.261
Expected:	Roll in [deg]	0.263	0.527	0.790	1.054
	Pitch in [deg]	3.885	5.495	6.729	7.771
	Yaw in [deg]	3.437	4.861	5.953	6.874

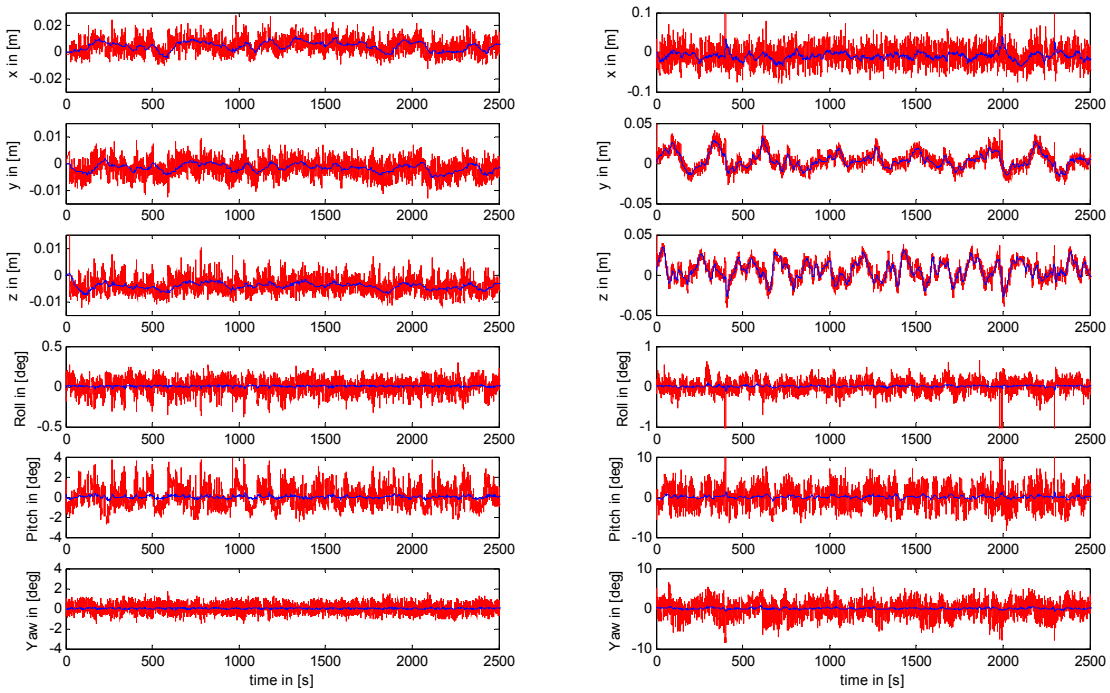

Fig. 11: *Position and attitude navigation error at 5m (left) and at 10m (right)*

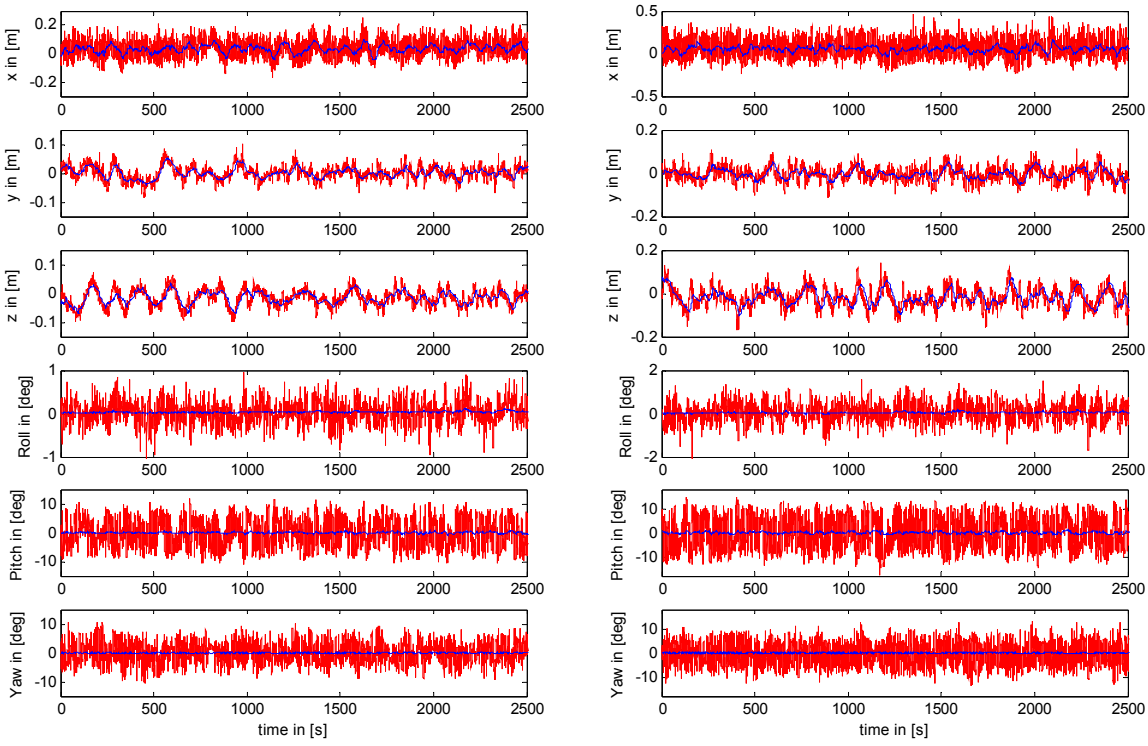

Fig. 12: *Position and attitude navigation error at 15m (left) and at 20m (right)*

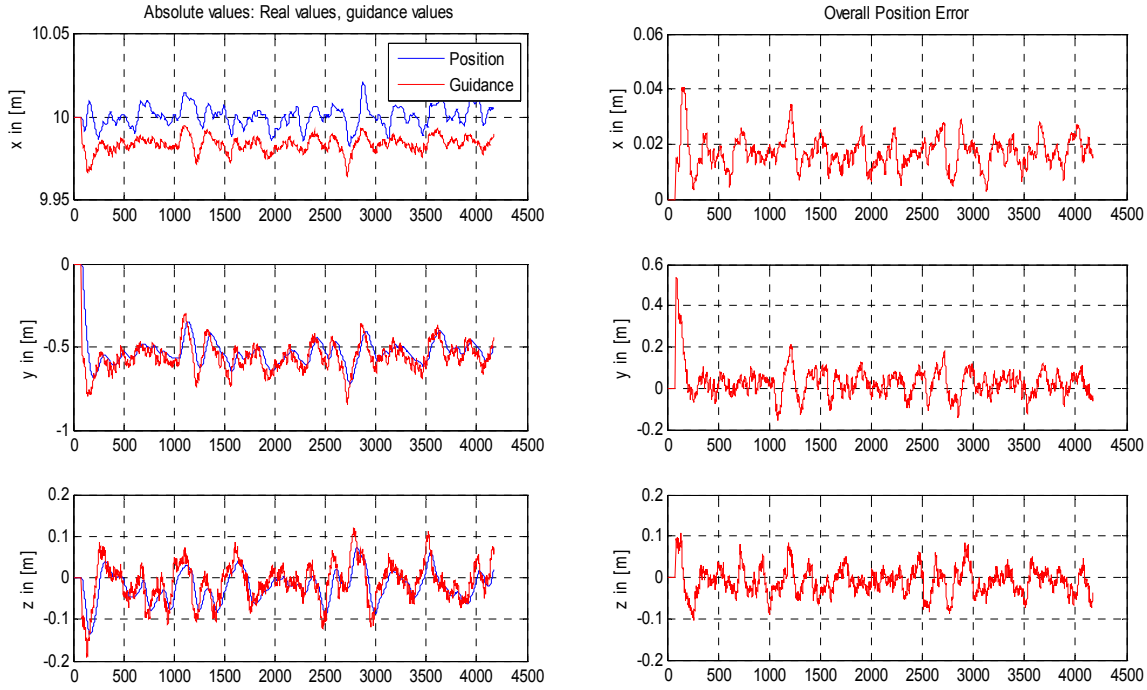

Fig. 13: *GNC System performance at 10m*

In addition to the navigation evaluation the complete GNC system performance has been investigated for the position control loop. In the following only the result of one demo test at 10m is presented. Fig. 13 shows the guidance function and the real trajectory of each component on the left side and on the right side the total performance error is displayed which is the difference between the real trajectory and the desired trajectory (guidance trajectory).
Summarized, the overall performance accuracy has a 3D value of better than 100mm. It is:

Position accuracy (@10m): 84.9mm

D. APPROACH SIMULATION

Furthermore an approach from a distance of 20m to a distance of 3m between chaser and target has been simulated. The hold point of 3m has been chosen due to the camera's field of view. A guidance trajectory similar with acceleration and deceleration phases is used for this simulation mode. The guidance function delivers a defined trajectory and forces a continuous approach.
Fig. 14 shows the x-coordinate of the resulting position vector. Measurement and filter as well as the real position are plotted. In addition on the ride side it presents the error of measurement (red) and Kalman filter estimates (blue) with respect to the distance.
The closed-loop simulation delivers stable values during the entire approach. One can observe a significant decrease in the noise with decreasing distance to the target. However, even big noise is well smoothed by the filter at all distances.

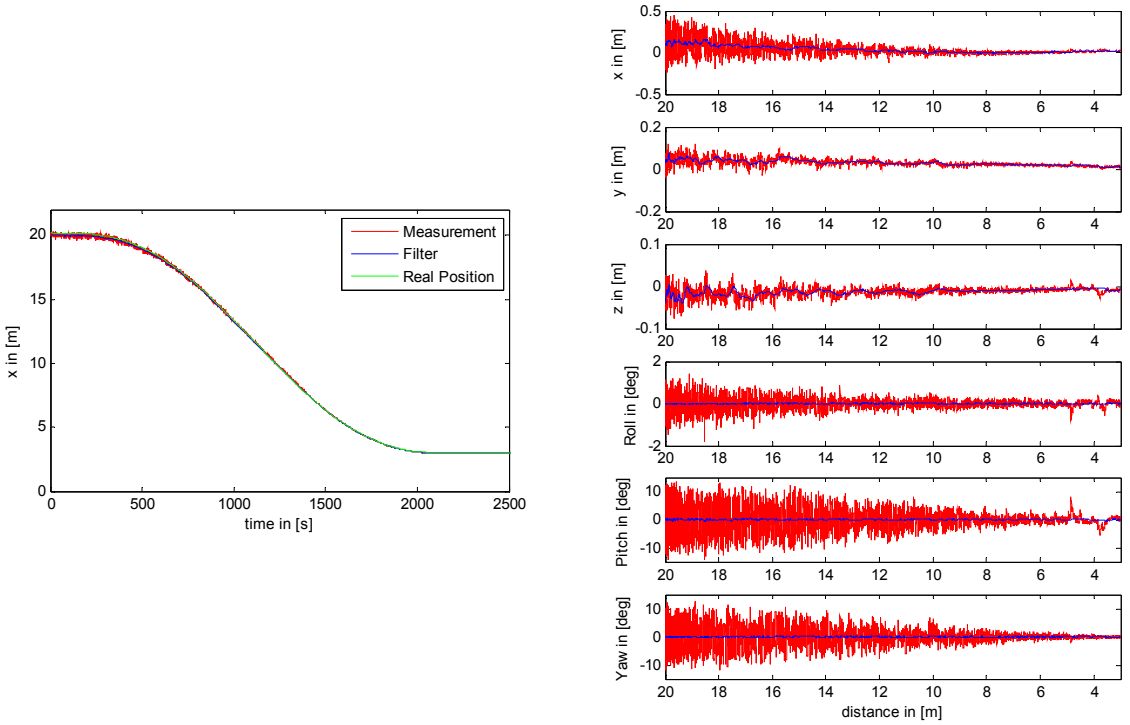

Fig. 14: *Results of approach simulation (left: x-coordinate of position measurement, filter estimates and real trajectory during, right: Position and attitude navigation errors)*

5. CONCLUSION AND OUTLOOK

This paper described the development of a rendezvous hardware-in-the-loop simulation using a vision-based sensor. The rendezvous scenario is based on the challenges of a new type of missions called On-Orbit Servicing missions which will use camera sensors to approach to a non cooperative client satellite. The new EPOS 2.0 facility at German Aerospace Center (DLR) is used to stimulate the sensor according to the numerical simulated trajectory.

First tests of the closed-loop rendezvous simulation have been successfully executed in real-time. The behavior at several hold points as well as during a continuous approach from 20m to 3m has been tested. The orbit and attitude control loop has been stable. The errors of the state estimates were in an acceptable range. They were compared by values derived from analytical calculations.

Several improvements and extensions of the current rendezvous simulation software could be done in the future. Currently, some work has already been started concerning camera calibration. Measurement errors are partly caused by the camera optics. The objective is to implement an online correction of radial and tangential distortion and skew.

Starting with these first rendezvous simulations, it needs to perform an extensive analysis of the single components and some optimization to improve their performance. In addition, a simulation with a scaled target model will be performed to extend the simulation distance virtually. Furthermore, the performance of the GNC system should be investigated under different illumination conditions.

6. REFERENCES

[1] T.A. Mulder, “Orbital Express Autonomous Rendezvous and Capture flight operations”, Part 1 of 2 and Part 2 of 2, *AIAA/AAS Astrodynamics Specialist Conference and Exhibit*, 18 - 21 August 2008, Honolulu, Hawaii

[2] R. Krenn, B. Schaefer, “Limitations of hardware-in-the-loop simulations of space robotics dynamics using industrial robots”, *European Space Agency*, ESA SP-440, Aug. 1999, pp. 681-686.

[3] S. Ananthakrishnan, R. Teders, and K. Alder, “Role of estimation in real-time contact dynamics enhancement of space station engineering facility”, *IEEE Rob. and Auto. Mag.*, Vol. 3(3), 1996, pp. 20-28.

[4] F.D. Roe, R.T. Howard, and L. Murphy, "Automated rendezvous and capture system development and simulation for NASA", *Proc. SPIE*, Vol. 5420, 118 (2004); doi:10.1117/12.542529
[5] J.-C. Piedboeuf, J. De Carufel, F. Aghili, and E. Dupuis, Task verification facility for the Canadian special purpose dextrous manipulator, *IEEE Int Conf on Rob and Auto,* Detroit, 1999, Vol. 3, pp. 1077–1083.
[6] O. Ma, J. Wang, S. Misra, M. Liu, "On the validation of SPDM task verification facility", *J. of Rob. Syst*., Vol.21(5), 2004, pp. 219-235.
[7] R. Bell et al., "Hardware-in-the-loop tests of an autonomous gn&c system for on-orbit servicing", *AIAA-LA Section/SSTC Responsive Space Conference* 2003.
[8] W. F. Xu, B. Liang, Y. S. Xu, C. Li and W. Y. Qiang, "A Ground Experiment System of Free-floating Space Robot for Capturing Space Target", *J. of Intell. and Rob. Syst.*, Vol.48(2), pp. 187-208, 2007.
[9] F. Terui, "Model based Visual relative Motion Estimation and Control of Spacecraft Utilizing Computer Graphics", *21st International Symposium on Space Flight Dynamics*, Toulouse, France, 2009.
[10] G. Arantes Jr, A. S. Komanduri, D. Bindel, and L. S. M. Filho, "Relative visual navigation system for on-orbit service", *1st Conference in Guidance, Navigation & Control in Aerospace EURO GNC*, Munich, 2011.
[11] C. Miravet, L. Pascual, E. Krouch, and J. M. del Cura, "An image-based sensor system for autonomous rendez-vous with uncooperative satellites", in 7th International ESA Conference on Guidance, Navigation & Control Systems, 2008.
[12] Boge, T., et al.: "Hardware in the loop Simulator for Rendezvous and Docking Maneuvers (Hardware in the Loop Simulator von Rendezvous und Docking Manoevern)", *German Aerospace Congress of DGLR*, Aachen, Germany, 2009.
[13] T. Tzschichholz, and T. Boge, "GNC systems development in conjunction with a RvD hardware-in-the-loop simulator", *4th International Conference on Astrodynamics Tools and Techniques*, Madrid, Spain, 2010.
[14] W. Fehse, *Automated Rendezvous and Docking of Spacecraft*, Cambridge Aerospace Series, Washington D.C., 2003.
[15] J. R. Wertz, *Attitude Determination and Control*, Kluwer Academic Publishers, Dordrecht, Boston, London, 2002.
[16] I. Sobel, G. Feldman, "A 3x3 isotropic gradient operator for image processing", *Pattern Classification and Scene Analysis*, 1973.
[17] A. Shahrokni, T. Drummond, P. Fua: "Texture Boundary Detection For Real-Time Tracking", *In proceedings of International Conference on Computer Vision*, Beijin, China, 2004
[18] M.A. Fischler, R.C. Bolles, "Random sample consensus (RANSAC): a paradigm for model fitting with applications to image analysis and automated cartography", *Commun. ACM, 24(6)*. 1981.
[19] J.J. Moré, "The Levenberg-Marquardt algorithm: Implementation and theory", G. A. Watson (ed.): *Numerical Analysis,* Dundee 1977, Lecture Notes Math. 630, 1978.
[20] P. Zarchan, H. Musoff, *Fundamentals of Kalman Filtering: A practical approach*, Progress in Astronautics and Aeronautics, Volume 190, 2000